Analytical Methods

Cite this: *Anal. Methods*, 2011, **3**, 2237

www.rsc.org/methods

PAPER

Biocompatible self-assembled monolayer platform based on (3-glycidoxypropyl)trimethoxysilane for total cholesterol estimation

Saurabh Kumar,[a] Jay Singh,[a] V. V. Agrawal,[a] Mahboob Ahamad[b] and B. D. Malhotra*[a]

Received 19th April 2011, Accepted 29th June 2011
DOI: 10.1039/c1ay05231d

An electrochemical cholesterol biosensor has been fabricated *via* covalent immobilization of cholesterol oxidase and cholesterol esterase (ChOx and ChEt) onto a biocompatible self assembled monolayer (SAM) of (3-glycidoxypropyl)trimethoxysilane (GPTMS) fabricated onto an indium tin oxide (ITO) electrode. The ChOx/GPTMS/ITO bioelectrode has been characterized using Fourier transform infrared spectroscopy (FTIR), contact angle measurements (CA), atomic force microscopy (AFM), electrochemical impedance spectroscopy (EIS), and cyclic voltammetry (CV) techniques. The results of the electrochemical response studies indicate that the ChOx-ChEt/GPTMS/ITO biosensing electrode can be used to estimate the total cholesterol from 1.5 to 6.1 mM, has sensitivity of 0.351 μA $(mg/dl)^{-1}$, and can be used more than 10 times with a shelf life of up to 10 weeks. The value of the Michaelis–Menten constant (K_m) observed as 0.43 mM reveals a strong binding to the biocompatible GPTMS organic platform and shows low interference effect. Further, this biosensor can be used to estimate the total cholesterol concentration in serum samples.

1. Introduction

The development of a cholesterol biosensor is of considerable importance due to the prevalence of cardiovascular diseases.[1] The total cholesterol concentration in human blood should be less than 200 mg dL^{-1} and should not exceed 239 mg dL^{-1}. The cholesterol in blood can be estimated using (1) the Lieberman-Burchard reaction, (2) colorimetry, (3) high performance liquid chromatography (HPLC), *etc.* However, these methods require pre-separation of serum and plasma to prevent optical (colorimetric) interference.[2,3] In this context, biosensors have been considered as very important since they have the potential to provide rapid and selective information. Therefore, an efficient, selective, and sensitive cholesterol sensor is urgently required. The immobilization of enzymes such as ChOx and ChEt onto an appropriate matrix is very important to fabricate an effective biosensor.[4] The performance of a biosensor depends on the surface properties of a matrix material, the availability of functional groups, the mode of enzyme immobilization, and the activity of the enzyme on the electrode surface.[5–8]

SAMs have recently become interesting matrices since these are easy to form and have excellent ordered arrangement and high reproducibility *etc.*[9–12] SAMs enable the formation of organic surfaces, whose composition, structure and properties can be varied rationally. SAMs also permit reliable control and provide biocompatible environment for biomolecules at a substrate surface.[13–15] Many systems including long-chain carboxylic acids ($C_nH_{2n}COOH$) and organosilane species ($RSiX_3$, R_2SiX_2 or R_3SiX, where R is an alkyl chain and X is a chloro or alkoxy group) have been used to fabricate SAMs.[16,17] Recently, monolayers of functionalized silanes and epoxysilanes have attracted much attention for anchoring biomolecules such as proteins, enzymes and DNAs.[18–20] These silanes can act as cross-linkers because they contain Si–O bonds that react with surface hydroxyl groups of metal oxides, glass, silicon, quartz *etc.* and pendant-functionalized hydrocarbon chains that can bind with organic materials and desired biomolecules. Therefore, SAM formation by silanization may provide a uniform layer onto a desired surface to obtain defined surface properties. Chrisey *et al.* have reported the application of trimethoxysilylpropyldiethylenetriamine and *N*-(2-aminoethyl)-3-aminopropyl-trimethoxysilane (AEAPTS) for covalent binding of DNA to a silicon (Si) surface.[21] Demirel *et al.* have used a poly (*N*-isopropylacrylamide) layer on a Si wafer as a DNA sensor.[22] Xia Zhong *et al.* have utilized two silane layers of a 2D-network of (3-mercaptopropyl)-trimethoxysilane (MPS) to self-assemble gold nanoparticles and glucose oxidase for fabricating a glucose biosensor.[23]

Silane-based SAMs fabricated onto an ITO coated glass plate have been found to show interesting physical and chemical properties such as stability, transparency, and conductivity and can be utilized for biosensor applications.[24] Liju Yang *et al.* have developed a SAM based epoxysilane biosensor based on the immobilization of affinity-purified antibodies for *E. coli* O157:

[a]*Department of Science and Technology Centre on Biomolecular Electronics, Biomedical Instrumentation Section, National Physical Laboratory, Dr K.S. Krishnan Marg, New Delhi, 110012, India; Fax: +91-011-45609310; Tel: +91-011-45609152. E-mail: bansi.malhotra@gmail.com*
[b]*Department of Biochemistry, Jamia Hamdard, New Delhi, 110062, India*

H7 detection.[25] Moore *et al.* have prepared 3-aminopropyl-trimethoxysilane silane onto ITO glass for DNA binding.[26] Ruan *et al.* have recently demonstrated the application of a (3-glycidoxypropyl)trimethoxysilane SAM by immobilizing *E. coli* antibodies onto an ITO surface to fabricate an immunosensor for *E. Coli* O157:H7 detection.[27] Arya *et al.* have fabricated a cholesterol sensor based on organic AEAPTS deposited onto the ITO surface.[28]

We report results of the studies relating to fabrication of the (3-glycidoxypropyl)trimethoxysilane (GPTMS) SAM onto ITO coated glass substrate for immobilization of ChOx and ChEt *via* epoxy-amine bonding for detection of free and total cholesterol.

2. Materials and methods

(i) Chemicals and reagents

ChOx (EC 1.1.36 from *pseudomonas fluorescens*) with specific activity of 2.4 U mg^{-1}, cholesterol esterase (EC 3.1.1.13 from *pseudomonas species*) with specific activity of 165 U mg^{-1}, 3-glycidoxypropyltrimethoxysilane (GPTMS), polidocanol, cholesterol and cholesterol oleate have been procured from Sigma-Aldrich (USA). All other chemicals are of analytical grade and have been used without further purification. The deionized water is from a Millipore water purification system. The pre-cleaned hydrolyzed indium-tin-oxide (ITO) glass plates have been used as substrates for preparation of the GPTMS monolayer.

(ii) Enzyme solution preparation

The solution of ChOx (4.8 U ml^{-1}) and ChEt (330 U ml^{-1}) is freshly prepared in phosphate buffer (50 mM, pH 7.0) prior to use. Cholesterol ester (cholesterol oleate) solution (500 mg dL^{-1}) is first dissolved in 1% polidocanol (Brij) as a surfactant by heating and gentle stirring resulting in a clear and colourless suspension and the final volume is made by addition of 0.9% NaCl solution. This stock solution is further diluted to prepare different working concentrations of cholesterol and cholesterol oleate solution. The stock solution of cholesterol is prepared in deionized water having 10% Triton X-100 and stored at 4 °C.

(iii) Fabrication of SAM of GPTMS and immobilization of ChOx and ChEt

The GPTMS SAM on a pre-cleaned ITO plate is prepared as reported elsewhere.[28] In brief, ITO plates are pre-cleaned with acetone, ethanol, and with copious amounts of de-ionized water. Further, ITO plates are immersed in a solution of $H_2O_2/NH_4OH/H_2O$ (1 : 1 : 5, v/v) for about 30 min at 80 °C, to obtain uniformly distributed OH groups on the ITO surface, after which these are thoroughly rinsed with de-ionized water and are dried. The electrodes are immersed in a 1% (v/v) solution of 3-glycidoxypropyl trimethoxysilane in toluene for about 18 h at room temperature (25 °C) to form an epoxysilane monolayer that has many active tail epoxy groups for reacting readily with protein amino groups.[29] The SAM formation electrode is subsequently rinsed with toluene and water to remove any physically absorbed epoxysilane from the surface and is then dried under a stream of nitrogen. ChOx and ChEt (10 μL) are covalently immobilized onto the GPTMS/ITO electrode *via* formation of a covalent bond between the epoxy group of silane (GPTMS) and the NH_2-terminal of the enzymes. The ChOx/GPTMS/ITO and ChOx-ChEt/GPTMS/ITO bioelectrodes are kept for about 4 h in a humid chamber at room temperature (25 °C) for binding of the desired enzymes (Scheme 1). The ChOx/GPTMS/ITO and ChOx-ChEt/GPTMS/ITO bioelectrodes thus formed are washed with phosphate buffer (50 mmol L^{-1}, pH 7.0) containing 0.9% NaCl and 0.05% Tween 20 to remove any unbound enzyme and is stored at 4 °C when not in use.

(iv) Characterization

Fourier transform infrared (FTIR) studies of GPTMS/ITO and ChOx/GPTMS/ITO bioelectrodes have been conducted using the spectrometer (PerkinElmer, Spectrum BX II) in transmission mode in the region of 400–4000 cm^{-1}. The contact angle measurements (DSA100, DSA/V 1.9, Kruss Germany) using the sessile drop method and atomic force microscopy (AFM, Veeco DICP2) studies have been used for characterization of both the GPTMS/ITO electrode and ChOx/GPTMS/ITO electrodes. The electrochemical behavior of the electrode has been studied using cyclic voltammetry and impedance measurements on an Autolab potentiostat/Galvanostat (Eco Chemie, Netherlands) using a three electrode cell with ITO as the working electrode, platinum (Pt) wire as the auxiliary electrode and a Ag/AgCl electrode as reference electrode in phosphate buffer (PBS, 50 mM, pH 7.0, 0.9% NaCl) containing 5 mM $[Fe(CN)_6]^{3-/4-}$. The AFM measurements have been performed using a Digital Instrument NanoScopeIIIa in tapping mode, to investigate the surface properties.

3. Results and discussion

(i) FTIR analysis

The FTIR spectra of GPTMS and the ChOx modified GPTMS bioelectrode are shown in Fig. 1. The peaks seen at 3848 and 3625 cm^{-1} from the GPTMS/ITO (curve a) electrode are due to the OH stretching mode. The stretching due to alkyl hydrogen is obtained at 2930 cm^{-1} and the corresponding bending vibrations can be seen around 1519 cm^{-1}. The band seen around 1680 cm^{-1} is due to the bending vibration of –OH on the ITO surface. The Si–O–Si asymmetric stretching vibration appears as a strong and broad band around 1054 cm^{-1}. The ether linkage in the glycidoxy group is known to absorb in the same region and it overlaps with the strong Si–O–Si absorption. The Si–OH asymmetric stretching vibration is seen at 850 cm^{-1}. The peak around 831 cm^{-1} is due to the symmetric Si–O–Si stretching vibration. The peaks seen at 571 and 456 cm^{-1} are attributed to the O–Si–O vibrations. The out of plane bending vibrations of the C–OH groups can be seen as a weak peak at 664 cm^{-1}.

The FTIR spectrum of the ChOx/GPTMS/ITO bioelectrode (curve b) shows a band in the 1069–975 cm^{-1} region assigned to the C–H in-plane deformation of the trimethoxysilane unit. The 1637 cm^{-1} peak is attributed to the amide linkage indicating ChOx immobilization. The broad absorption peaks seen in the 3200–3350 cm^{-1} range are due to the O–H and N–H stretching vibration of epoxy-amine bond conforming immobilized ChOx.

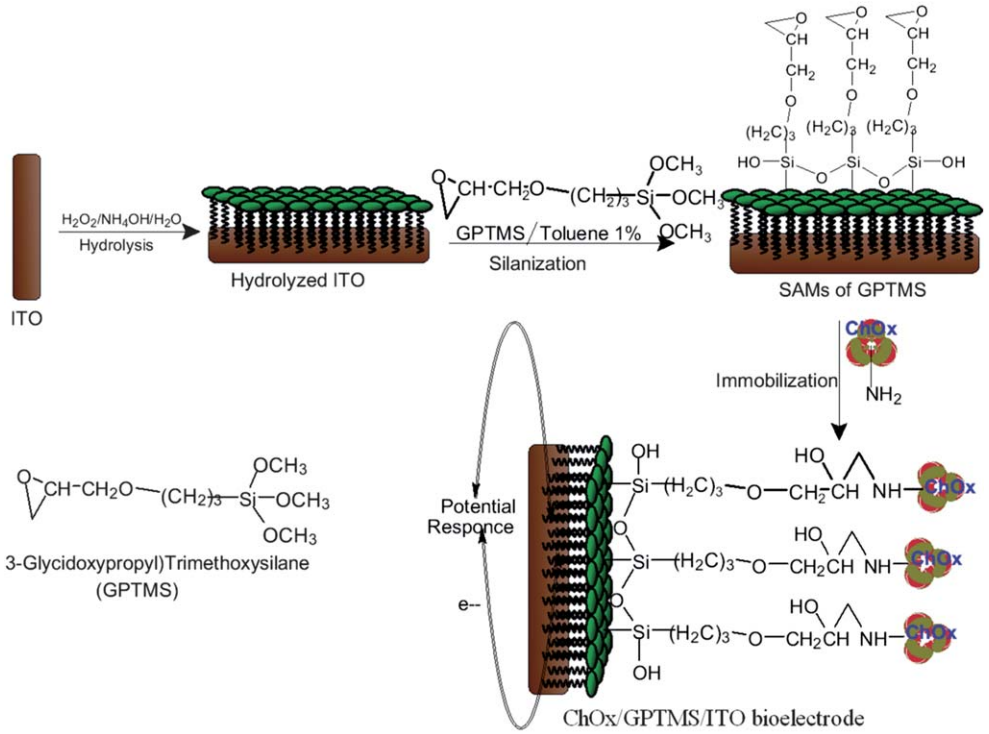

Scheme 1 The schematic of the covalent immobilization of ChOx onto the GPTMS/ITO surface.

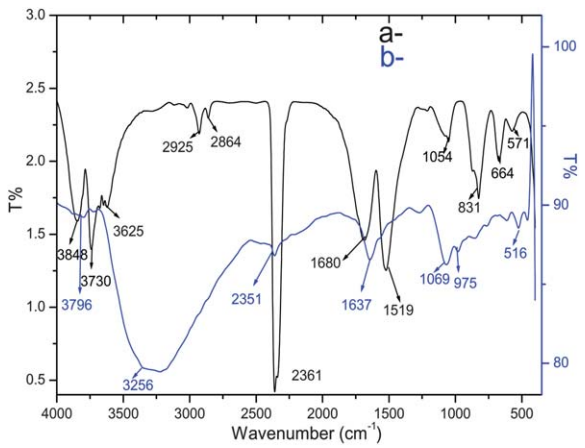

Fig. 1 FTIR spectra of (a) GPTMS/ITO electrode and (b) ChOx/GPTMS/ITO bioelectrode.

(ii) Contact angle studies

Contact angle (CA) measurements have been carried out to investigate the hydrophilic/hydrophobic character of the SAM surface. The CA value of hydrolyzed ITO, 48.22°, (Fig. 2A) increases to 69.19° (Fig. 2B) revealing the fabrication of the GPTMS monolayer onto the hydrolysed ITO. The increase in CA can be attributed to the presence of the hydrophobic epoxy group present in GPTMS. The contact angle decreases to 13° (Fig. 2C) after the immobilization of ChOx. The decrease in the value of the contact angle is attributed to the hydrophilic nature of the surface and thus confirms the immobilization of ChOx on the GPTMS/ITO electrode surface.

(iii) Atomic force microscopic (AFM) measurements

The AFM image of the GPTMS/ITO electrode (Fig. 3A) exhibits a spindle-like structure revealing GPTMS-SAM formation with surface roughness of 7 nm. The distribution of the GPTMS monolayer on the ITO surface is uniform, dense, and homogenous with only a few homogeneous aggregates. Fig. 3B shows the topography of the ChOx/GPTMS/ITO bioelectrode indicating the homogeneity effect and a height of about 10 nm, indicating the immobilization of ChOx. The change in morphology of the ChOx/GPTMS/ITO bioelectrode can be attributed to the presence of ChOx on GPTMS. The globular structure and bigger size of ChOx attached onto the GPTMS/ITO electrode *via* covalent binding is clearly visible. Covalent binding of ChOx with functional moieties of the GPTMS in an alike fashion indicates that ChOx molecules are more compact at the GPTMS-SAM/ITO electrode.

(iv) Biocompatibility test of GPTMS-SAM

The biocompatibility of GPTMS has been investigated with both bacterial culture (*E.coli* DH5α, Gram negative bacteria) and plant tissue culture (wheat seed). For the bacterial system, *E.coli* is grown for 24 h in nutrient broth medium at 37 °C in a rotary shaker at 100 rpm, after which 100 μL of culture is spread and 4 wells (5 mm each under sterile conditions) on a nutrient agar petriplate are made. 25 μL solution of the GPTMS (2%, 1%, 0.1%, and 0.01% in toluene) is added to each well, and is kept overnight at 37 °C. After 24 h incubation, the control shows the zone of growth retardation whereas different concentrations of GPTMS reduce the zone of bacterial growth inhibition indicating the biosafety of GPTMS on the bacterial culture (Fig. 4A). For plant germination, the wheat seed surface is sterilized by the

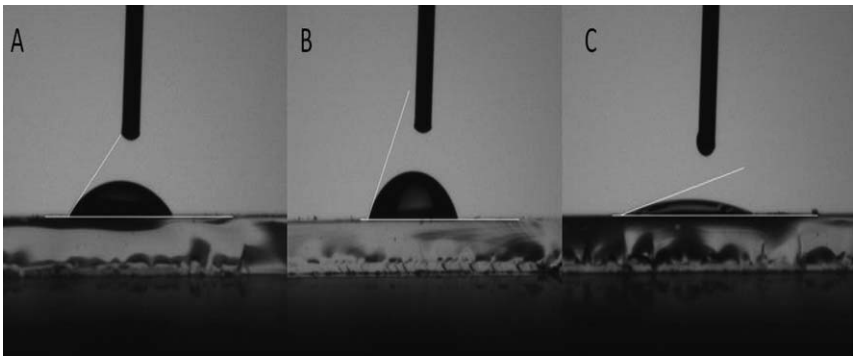

Fig. 2 Contact angle measurement of (A) hydrolyzed ITO, (B) GPTMS/ITO electrode and (C) ChOx/GPTMS/ITO bioelectrode.

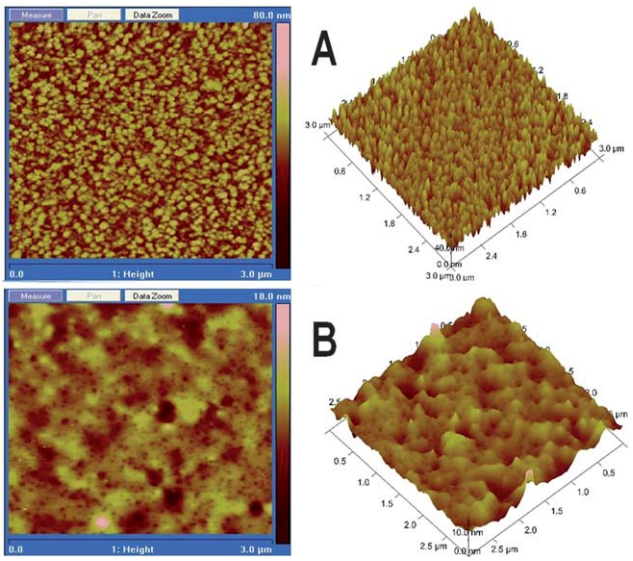

Fig. 3 Two dimensional and three dimensional AFM image of (A) GPTMS/ITO electrode and (B) ChOx/GPTMS/ITO bioelectrode in 3 μm × 3 μm.

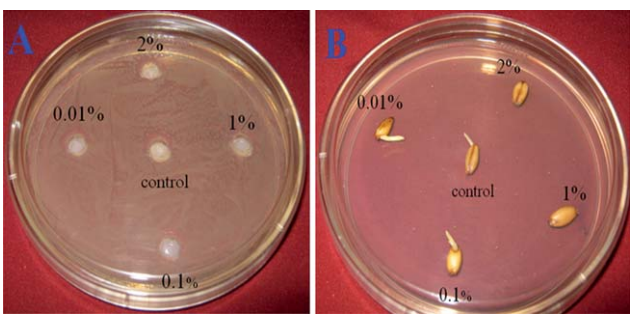

Fig. 4 Snapshot of the agar plates containing (A) *E.Coli* sp. after 24 h of incubation, revealing no inhibition zone formation in the plate using GPTMS solution and (B) wheat seeds after 2 days of incubation, revealing proper seed germination, showing the biocompatibility of GPTMS.

following process. Wheat seed is treated with 2 drops of Tween-80 (detergent) in distilled water (DW) for about 10 min, is then washed multiple times with DW, after which 70% ethyl alcohol (2 min), 0.1% mercuric chloride (5 min) are added, followed by rinsing with copious amounts of sterilized deionized water. The wheat seeds are then immersed in different concentrations of SAM of the GPTMS solution (2%, 1%, 0.1%, and 0.01%) and are placed on the solid agar media (where plants get nutrients) and are incubated at room temperature for 48 h. Seed germination is not clearly visible in 1% and 2% due to a delay in seed germination. It is perhaps the increased concentration of the GPTMS molecule that results in delayed seed germination.

Fig. 4B shows the image of GPTMS-SAM obtained after seed germination and the result reveals appropriate seed germination in almost all the concentrations of the plant tissue culture, indicating the biocompatible nature of the GPTMS-SAM.

(v) Electrochemical impedance spectroscopy

At the electrode/solution interface the charge transfer phenomenon has been investigated using the electrochemical impedance technique (EIS). The results of EIS measurements indicate hindrance provided by the GPTMS layer to the transfer of charge from solution to the electrode due to the insulating nature of epoxysilane that inhibits the permeability of $[Fe(CN)_6]^{3-/4-}$ to the surface of the electrode.[30] Thus, the change in the charge transfer resistance (R_{CT}) value can be correlated with the modified surface. Fig. 5 shows the charge transfer resistance (Nyquist diameter) of

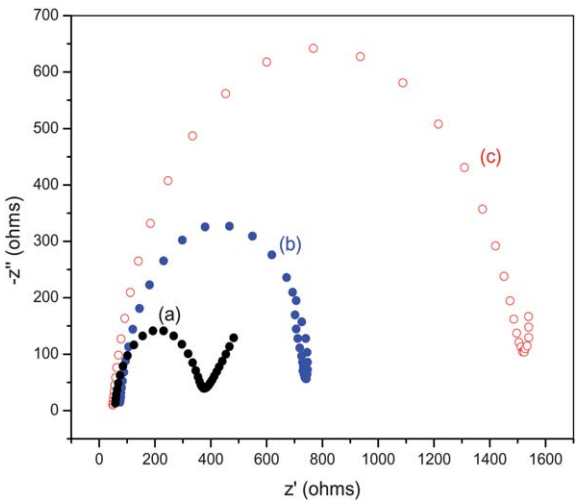

Fig. 5 Impedance spectra of (a) hydrolyzed ITO, (b) GPTMS/ITO electrode and (c) ChOx/GPTMS/ITO bioelectrode.

hydrolyzed ITO (a), GPTMS/ITO (b) and the ChOx/GPTMS/ITO bioelectrode (c). The value of R_{CT} for GPTMS/ITO (668.55 ohms, curve b) is found to be higher than that of the ITO electrode (311.67, curve a). This suggests that deposition of GPTMS SAM onto the ITO surface hinders the electrode transfer kinetics between the electrolyte and the ITO electrode revealing fabrication of the SAM. The value of R_{CT} (1467.53 ohms, curve c) for the ChOx/GPTMS/ITO bioelectrode is larger than that of the GPTMS/ITO electrode (R_{CT} 668.55 ohms). The increase in the value of R_{CT} is attributed to the hindrance caused by the macromolecular structure of ChOx to the electron transfer. This increase in the value of R_{CT} on the immobilization of the enzyme (ChOx) further confirms the immobilization of the enzyme.

(vi) Cyclic voltammetric studies

Fig. 6A shows the cyclic voltammograms (CV) obtained for hydrolyzed ITO (a), GPTMS/ITO electrode (b) and ChOx/GPTMS/ITO bioelectrode (c). The decrease in the value of the electrochemical response current of the GPTMS/ITO electrode than that of hydrolyzed ITO electrode indicates the formation of a SAM of GPTMS onto the ITO surface. The decrease in the electrochemical response current value can be attributed to the non-conducting nature of the GPTMS-SAM on the ITO surface that inhibits the permeability of the redox couple $[Fe(CN)_6]^{3-/4-}$ towards the ITO electrode. The decrease in the value of the oxidation current observed after immobilization of ChOx onto the GPTMS/ITO electrode is attributed to the hindrance caused by the macromolecular structure of ChOx to the electron transport indicating immobilization of the ChOx.

Fig. 6B shows the results of CV studies obtained for the ChOx/GPTMS/ITO bioelectrode in PBS (50 mM, pH 7.0, 0.9% NaCl) containing 5 mM redox couple $[Fe(CN)_6]^{3-/4-}$ as a function of scan rate from 50 to 100 mV s^{-1}. It can be seen that the peak-to-peak potential ($\Delta E = E_a - E_c$) and magnitude of the current [both anodic (I_a) and cathodic (I_c)] exhibits a linear relationship with the square of the root of the scan rate (inset, Fig. 6B) indicating that the electrode undergoes uniform facile charge transfer kinetics and reversible electron transfer kinetics, according to eqn (1)–(3).

$$\Delta E\,(\mathrm{V})\,(\mathrm{ChOx/GPTMS/ITO\ bioelectrode}) = 0.2\,(\mathrm{V}) + 0.421\,(\mathrm{s}) * \text{scan rate}\,(\mathrm{mV\ s^{-1}})\ \text{with regression coefficient} = 0.998 \quad (1)$$

$$I_a\,(\mathrm{ChOx/GPTMS/ITO\ bioelectrode}) = 120.9\ \mu + 94.6\ \mu * \text{scan rate}\,(\mathrm{mV\ s^{-1}})\ \text{with regression coefficient} = 0.997 \quad (2)$$

$$I_c\,(\mathrm{ChOx/GPTMS/ITO\ bioelectrode}) = 130\ \mu + 50.8\ \mu * \text{scan rate}\,(\mathrm{mV\ s^{-1}})\ \text{with regression coefficient} = 0.998 \quad (3)$$

GPTMS-SAM provides covalent bonding to immobilized biomolecules (ChOx and ChEt) and acts as a molecular wire between biomolecules and the electrode surface. Besides this, GPTMS-SAM is one molecule thick and hence it provides easier access to the analyte (cholesterol molecule) for faster transfer of charges due to the molecular interaction between the analyte and biomolecules being near the vicinity of electrode surface resulting in higher sensitivity of the fabricated bioelectrode.

The optimization of working pH for the enzyme electrode is considered to be important because ability of amino acids

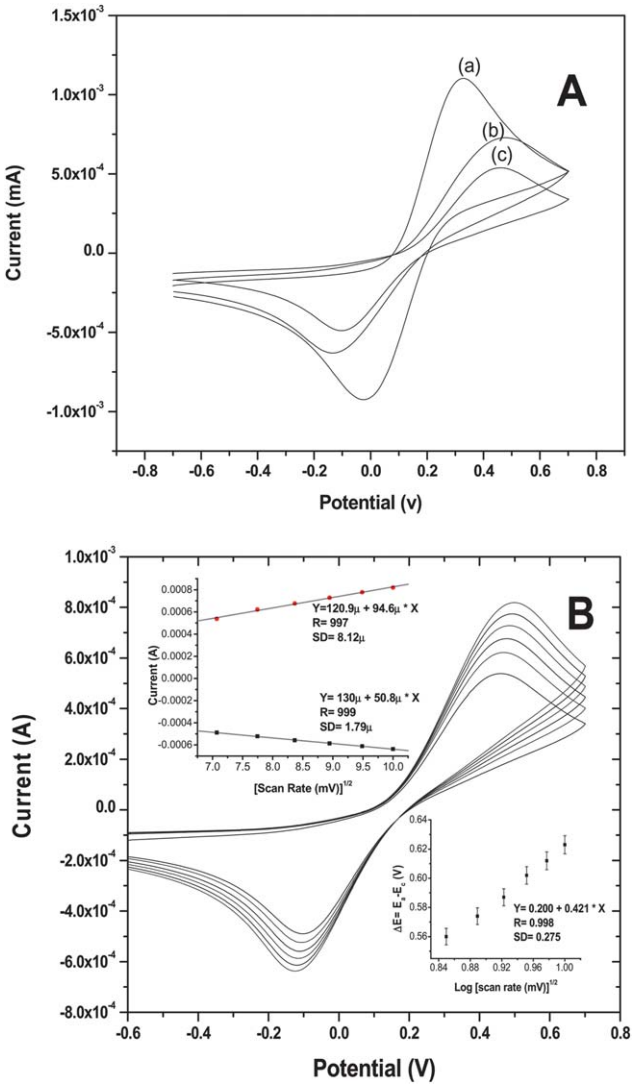

Fig. 6 (A): Cyclic votammograms for (a) ITO surface, (b) GPTMS/ITO electrode, (c) ChOx/GPTMS/ITO bioelectrodes in three-electrode configuration with Ag/AgCl electrode as a reference electrode in PBS solution (50 mM, pH 7.0, 0.9% NaCl). (B) Cyclic voltammograms (CV) of ChOx/GPTMS/ITO bioelectrode as a function of scan rate, Inset a: curve between I (A) and square root of scan rate (mV s^{-1}), Inset b: curve between E (V) and logarithm of scan rate (mV s^{-1}).

present at the active sites of the enzyme to interact with the substrate depends on the electrostatic interaction which in turn depends on the pH of the solution. To find the optimal pH, the activity of the ChOx/GPTMS/ITO bioelectrode can be measured in the pH range of 6.0 to 8.0 at 25 °C (data not shown). The optimum current is obtained at pH 7.0. Hence all experiments have been conducted at pH 7.0 at which the natural structures of biomolecules are retained.

(vii) Response studies of the ChOx-ChEt/GPTMS/ITO bioelectrode

The electrochemical response characteristics of the ChOx/GPTMS/ITO bioelectrode (Fig. 7A) have been conducted as a function of cholesterol concentration (25–400 mg dl^{-1}) in PBS

(50 mM, pH 7.0, 0.9% NaCl) containing 5 mM $[Fe(CN)_6^{3-/4-}]$ for the 60 s. The biochemical reaction (Scheme. 2) involved in the electrochemical measurements is:

$$\text{Cholestrol Oleate} + H_2O \xrightarrow{\text{ChEt}} \text{Cholestrol} + \text{Fatty acid} \quad ((i))$$

$$\text{ITO-GPTMS-ChOx}_{oxi} + \text{Cholestrol} + O_2 \rightarrow \text{ITO-GPTMS-ChOx}_{red} + \text{4-cholesten-3-one} + H_2O_2 \quad ((ii))$$

$$H_2O_2 \xrightarrow{\text{Electrochemical oxidation}} 2H^+ + O_2 + 2e^- \quad ((iii))$$

Fig. 7A shows the variation of the electrochemical response current recorded for the ChOx/GPTMS/ITO bioelectrode as a function of free cholesterol concentration. The increase in the value of oxidation current with the increase in cholesterol concentration indicates an increase in the concentration of H_2O_2 (as shown in Fig. 7). The bioelectrode follows enzyme kinetics {Inset Fig. 7A (i)}; at relatively low concentrations of cholesterol, the current increases almost linearly with an increased cholesterol concentration but at higher cholesterol concentration

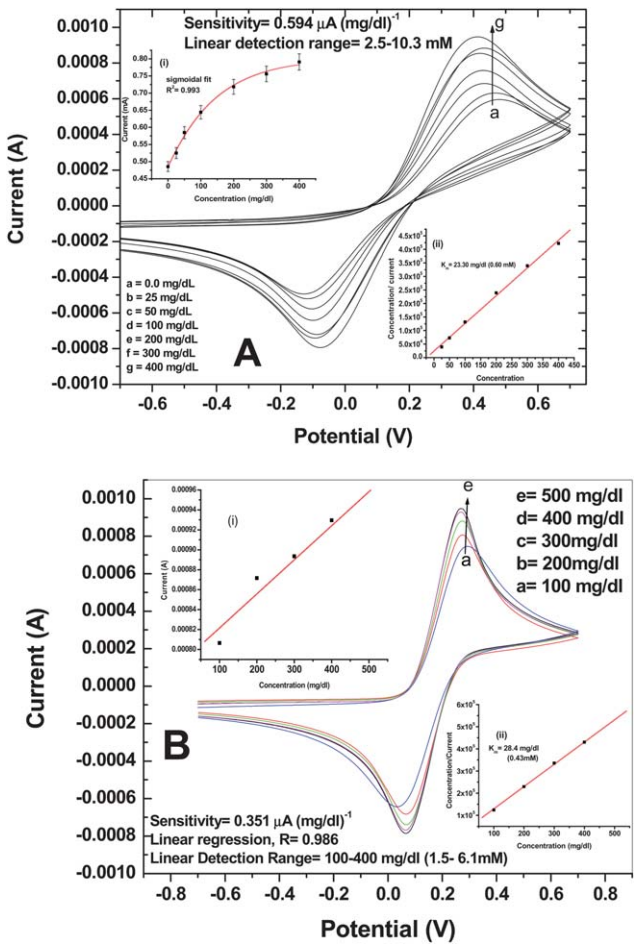

Fig. 7 (A and B): Electrochemical response of the ChOx/GPTMS/ITO and ChOx-ChEt/GPTMS/ITO bioelectrode at different concentration of cholesterol, 25, 50, 100, 200, 300, 400 mg dl^{-1}, at a scan rate of 50 mV s^{-1}. Inset: Calibration plot between the magnitude of current (mA) and cholesterol concentration (mg dl^{-1}) (Boltzman fit, $R_2 = 0.996$, inset i). (Inset ii): Hanes plot of covalently immobilized ChOx and ChEt onto GPTMS of SAM.

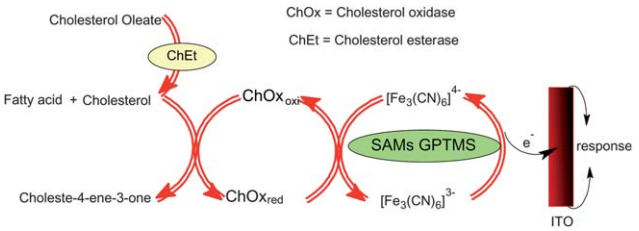

Scheme 2 Schematic illustration of the biochemical reaction at the ChEt-ChOx/GPTMS/ITO bioelectrode.

the current increases by a smaller magnitude. The linearity is found from 100 to 400 mg dl^{-1} (2.58–10.34 mM). The sensitivity of the ChOx/GPTMS/ITO bioelectrode estimated from the slope of the curve has been found to be 0.594 μA $(mg/dl)^{-1}$. The enzyme–substrate kinetic parameter (Michaelis–Menten constant, K_m) can be estimated from the Hanes Plot {inset Fig. 7A (ii)}, between cholesterol concentrations and cholesterol concentration/current. The value of K_m for the ChOx/GPTMS/ITO bioelectrode is found to be 0.60 mM indicating a high affinity for cholesterol in the immobilization of ChOx to

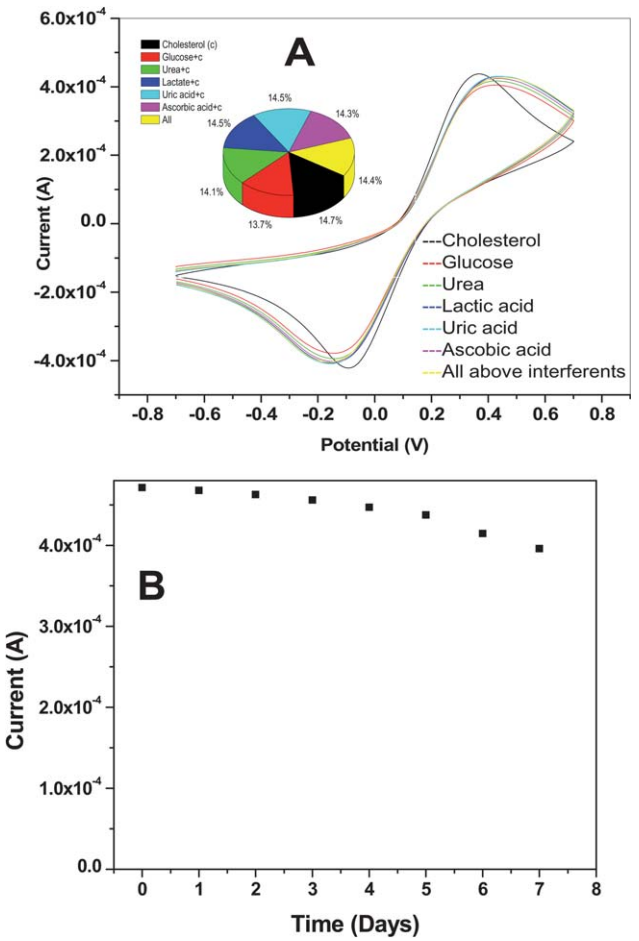

Fig. 8 (A) The effect of interferents on the electrochemical response of the ChOx/GPTMS/ITO bioelectrode (inset % effect of interferents. (B) Shelf-life curve for the ChOx/GPTMS/ITO bioelectrode as a function of time.

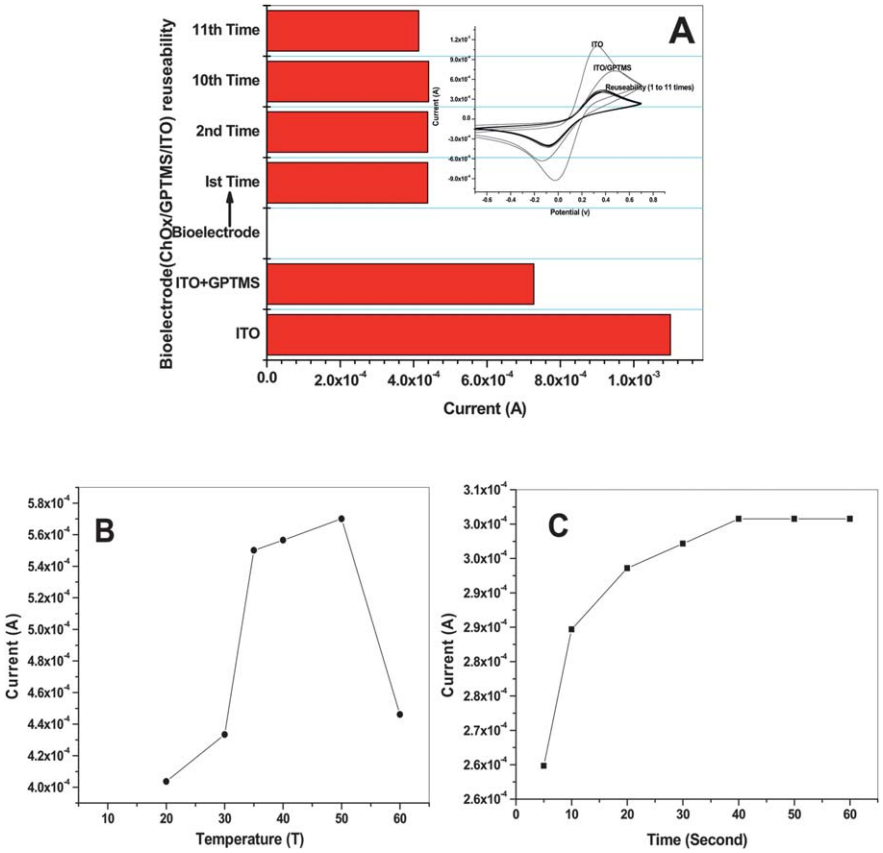

Fig. 9 (A) Electrochemical representation of the ChOx/GPTMS/ITO bioelectrode reuseability. Inset: showing CV of ITO, GPTMS/ITO electrode and ChOx/GPTMS/ITO (multitime use) bioelectrode. (B) Effect of temperature on ChOx/GPTMS/ITO bioelectrode. (C) Electrochemical response time from 5 to 60 s incubation period.

GPTMS. The highest catalytic turnover is obtained at a relatively low substrate concentration for the enzyme with a small value of K_m.

Fig. 7B shows the value of total cholesterol by using the ChOx-ChEt/GPTMS/ITO bioelectrode under similar reaction conditions. It can be seen that the bioelectrode has linearity between 100–400 mg dl^{-1} {inset Fig. 7B (i)} with regression coefficient ($R = 0.986$). The sensitivity and K_m value of the ChOx-ChEt/GPTMS/ITO bioelectrode are found to be 0.351 μA $(mg/dl)^{-1}$, 28.4 mg dl^{-1} (0.43 mM) {inset Fig. 7B (ii)}, respectively.

(viii) Self-life and effect of interferents

The selectivity of the ChOx/GPTMS/ITO bioelectrode has been determined by measuring the electrochemical response while adding normal concentrations of different interferents (Fig. 8A), such as glucose (5 mM), urea (1 mM), lactic acid (0.5 mM), uric acid (0.1 mM) and ascorbic acid (0.05 mM) in phosphate buffer (50 mM, pH 7.0, 0.9% NaCl) containing 5 mM $[Fe(CN)_6]^{3-/4-}$ at 50 mV s^{-1} scan rate. The deviation of response has been calculated according to $(I_i - I_g)/I_g$, where I_i and I_g are the steady-state currents recorded for PBS containing equal amounts (1 : 1) of cholesterol (200 mg dl^{-1}) and interferent. The electrochemical response studies indicate that the results of value of the current decreases by a negligible amount. Interference studies of the ChOx/GPTMS/ITO electrode are represented by a pie chart (Inset: Fig. 8A). The value of the current obtained in the bioelectrode in the presence of cholesterol is 14.7% and the maximum interference of the current in the presence of glucose is 1%. However, it is 0.2% in presence of lactic and uric acid respectively.

Table 1 Determination of cholesterol in serum samples by ChOx/GPTMS/ITO bioelectrode

Cholesterol concentration (mg/dL)	Value of current obtained with serum sample (mA)	Value of current obtained for pure cholesterol sample (mA)	% RSD
155	0.3886	0.3503	10.9
190	0.4012	0.3942	1.77
214	0.4058	0.3966	2.32
257	0.4172	0.3854	8.25
280	0.4076	0.3902	4.47

Table 2 Determination of cholesterol in serum samples by ChEt-ChOx/GPTMS/ITO bioelectrode

Cholesterol concentration (mg/dL)	Value of current obtained with serum sample (mA)	Value of current obtained for cholesterol oleate sample (mA)	% RSD
131	0.5493	0.5300	3.6
167	0.5678	0.5430	4.5
184	0.5246	0.5536	5.2
195	0.5682	0.5619	1.1
214	0.5757	0.5756	0.01
236	0.6018	0.6010	0.13

Table 3 Characteristics of the ChOx-ChEt/GPTMS/ITO bioelectrode and others reported in the literature for total cholesterol estimation

S. N	Immobilization matrix	Sensing element	Method of immobilization	Linearity	Transducer used	K_m (mM)	Sensitivity and shelf life	Reference
1	MWNTs	ChOx, ChEt, HRP	Physical entrapment	100–400 mg dl^{-1}	Amperometry	—	0.0059 μA $(mg/dl)^{-1}$	33
2	Thiotic acid/gold	ChOx, ChEt	Biotin-avidin	1–6 mM	Square wave voltammetry	—	69 nA mM^{-1}, 10 days	34
3	*N*-(2-aminoethyl)-3-aminopropyltrimethoxysilane	ChOx, ChEt, HRP	Covalent	0.15–7.68 mM	Spectrophotometric and electrochemical (CV)	1.46	124 nA $(mg/dl)^{-1}$, 10 weeks	35
4	GPTMS SAM	ChOx, ChEt	Covalent	100–400 mg dl^{-1}	Cyclic voltametry	0.43	0.351 μA $(mg/dl)^{-1}$, 10 weeks	Present work

The shelf-life of the ChOx/GPTMS/ITO bioelectrode has been monitored by measuring the electrochemical current response with respect to time, with regular intervals of 1 day as shown in (Fig. 8B). It is observed that this bioelectrode retains about 85% of enzyme (ChOx) activity even after about 9 days when stored in refrigerated conditions (4 °C) and after which the current response decreases up to 72% in about 10 weeks (data not shown). For activity measurements, a temperature of 30 °C and a ChOx concentration of 200 mg dl^{-1} are used.

(ix) Effect of temperature, reusability, response time and serum sample analysis of the ChOx/GPTMS/ITO bioelectrode

Fig. 9A shows the electrochemical bar plot of reusability measuring at 200 mg dl^{-1} cholesterol concentration in PBS (50 mM, pH 7.0, 0.9% NaCl) containing 5 mM $[Fe(CN)_6^{3-/4-}]$ indicating that the ChOx/GPTMS/ITO bioelectrode can be used more than 10 times. The activity of the ChOx/GPTMS/ITO bioelectrode has been measured as a function of temperature varying from 20 to 60 °C (Fig. 9B). It is observed that the value of response current increases with increasing the temperature up to 50 °C. The higher thermal stability of the ChOx/GPTMS/ITO bioelectrode can be attributed to the epoxy SAM acting as a pillar which retains the biological conformation of the enzyme at higher temperatures. For the determination of the response time we have measured the electrochemical response current from 5 to 60 s as shown in Fig. 9C. The magnitude of the current increases initially (5 to 40 s) and after 40 s the current becomes almost constant indicating that 40 s is the response time of the ChOx/GPTMS/ITO bioelectrode.

Traditionally, cholesterol is determined by using a non-enzymatic spectroscopic technique using colored substances.[31] This method usually involves a complex procedure for the precipitation of lipoprotein fractions and suffers from low specificity, instability of reagents compounded with high cost and standardization difficulties. Hence, it is desirable to develop techniques for the cost-effective, convenient, rapid and sensitive estimation of cholesterol. Enzymatic methods offer selectivity, specificity and high sensitivity for the determination of cholesterol.[32] Therefore attempts have been made to estimate the total cholesterol concentration present in serum samples by using the ChEt-ChOx/GPTMS/ITO bioelectrode. Serum samples of known concentration have been obtained from a clinic located in New Delhi. It can be seen that magnitude of the current obtained with serum samples and pure cholesterol samples is reasonable (Table 1 and 2.). Table 3 shows the characteristics of cholesterol biosensor based on the ChOx-ChEt/GPTMS/ITO electrode, including those reported in the literature.[33–35]

4. Conclusions

We have fabricated an electrochemical cholesterol biosensor *via* covalent immobilization of ChOx and ChEt onto a GPTMS-SAM fabricated onto ITO. The fabricated ChOx-ChEt/GPTMS/ITO bioelectrodes exhibit high sensitivity of 0.351 μA $(mg/dl)^{-1}$ and a linearity range of 100–400 mg dl^{-1} with detection limit as 90.7 mg dl^{-1} of total cholesterol concentration. The low K_m value of 0.43 mM indicates that the bioelectrode has a high enzyme affinity towards ChOx and ChEt. The stability of the bond between the specific functional group of ChOx and GPTMS-SAM on the ITO electrode surface results in increased thermal stability of the bioelectrode up to about 50 °C. The shelf-life of the electrode is found to be approximately 10 weeks when stored at 4 °C, and the electrode can be reused more than 10 times with 40 s as the response time. Moreover, this biosensor virtually minimizes the effect of interference and can be useful to detect total cholesterol in real serum samples containing other analytes. Efforts should be made to improve the detection limit of the biocompatible GPTMS-SAM platform for cholesterol detection for *in vitro* sensing. The results of these studies have implications

towards the application of this biocompatible platform towards *in vivo* sensing.

Acknowledgements

We thank Prof. R. C. Budhani, Director, NPL, India for the facilities. Financial support received from the Department of Science and Technology (DST/TSG/ME/2008/18), Department of Biotechnology (BT/PR 7667/MED/14/1057/2006) and Council of Scientific and Industrial Research (CSIR), India is sincerely acknowledged.

References

1 M. Nauck, W. März and H. Wieland, *Clin. Chem.*, 2000, **46**, 436.
2 M. N. Nanjee and S. M. Markovina, *Clin. Chem.*, 1996, **42**, 915.
3 Y. Hirowatari, H. Yoshida, H. Kurosava, K. Doumito and N. Tada, *J. Lipid Res.*, 2003, **44**, 1404.
4 A. Kumar, Rajesh, A. Chaubey, S. K. Grover and B. D. Malhotra, *J. Appl. Polym. Sci.*, 2001, **82**, 3486.
5 A. Li, F. Yang, Y. Ma and X. Yang, *Biosens. Bioelectron*, 2007, **22**, 11722.
6 Y. H. Song, L. Wang, C. B. Ren, G. Y. Zhu and Z. Li, *Sens. Actuators, B*, 2006, **114**, 1001.
7 W. Limbutt, P. Kanatharana, B. Matisson, P. Asawatreratanakul and P. Thavarungkul, *Anal. Chim. Acta*, 2006, **561**, 55.
8 M. Gerard, K. Ramanathan, A. Chaubey and B. D. Malhotra, *Electroanalysis*, 1999, **11**, 450.
9 Anees A. Ansari, A. Kaushik, P. R. Solanki and B. D. Malhotra, *Electrochem. Commun.*, 2008, **10**, 1246.
10 T. Nakaminami, S. Ito, S. Kuwabata and H. Yoneyama, *Anal. Chem.*, 1999, **71**, 1068.
11 K. V. Gobi and F. Mizutani, *Sens. Actuators, B*, 2001, **80**, 272.
12 H. Zhao and H. Ju, *Anal. Biochem.*, 2006, **350**, 138.
13 K. Wadu-Mesthrige, N. A. Amro and G. Y. Liu, *Scanning*, 2000, **22**, 380.
14 S. Ferrett, S. Paynter, D. A. Russell and K. E. Sapsford, *TrAC, Trends Anal. Chem.*, 2000, **19**, 530.
15 S. Dong and J. Li, *Bioelectrochem. Bioenerg.*, 1997, **42**, 7.
16 N. K. Chaki and K. Vijayamohanan, *Biosens. Bioelectron.*, 2002, **17**, 1.
17 R. K. Smith, P. A. Lewis and P. S. Weiss, *Prog. Surf. Sci.*, 2004, **75**, 1.
18 V. R. S. Babu, M. A. Kumar, N. G. Karnath and M. S. Thakur, *Biosens. Bioelectron.*, 2004, **19**, 1337.
19 F. Nakamura, E. Ito, Y. Sakao, N. Ueno, I. N. Gatuna, F. S. Ohuchi and M. Hara, *Nano Lett.*, 2003, **3**, 1083.
20 T. Nakagawa, T. Tanaka, D. Niwa, T. Osaka, H. Takeyama and T. Matsunaga, *J. Biotechnol.*, 2005, **116**, 105.
21 L. A. Chrisey, G. U. Lee and C. E. O'Ferrall, *Nucleic Acids Res.*, 1996, **24**, 3031.
22 G. Demirel, Z. Rzaev, S. Patir and E. Pişkin, *J. Nanosci. Nanotechnol.*, 2009, **9**, 1865.
23 X. Zhong, R. Y. Y. Chai, Y. Liu, J. Dai and D. Tang, *Sens. Actuators, B*, 2005, **104**, 191.
24 H. Hillebrandt and M. Tanaka, *J. Phys. Chem. B*, 2001, **105**, 4270.
25 L. Yang and Y. Li, *Biosens. Bioelectron.*, 2005, **20**, 1407.
26 E. Moore, D. O'Connell and P. Galvin, *Thin Solid Films*, 2006, **515**, 2612.
27 C. Ruan, L. Yang and Y. Li, *Anal. Chem.*, 2002, **74**, 4814.
28 S. K. Arya, A. K. Prusty, S. P. Singh, P. R. Solanki, M. K. Pandey, M. Datta and B. D. Malhotra, *Anal. Biochem.*, 2007, **363**, 210.
29 C. Hao, F. Yan, L. Ding, Y. Xue and H. Ju, *Electrochem. Commun.*, 2007, **9**, 1359.
30 K. Takehara, H. Takemura and Y. Ide, *Electrochim. Acta*, 1994, **39**, 817.
31 A. Gavarro, E. Berlangu, F. Campose, A. Veragaus, C. Lliminana, T. Torra, *Proceedings of the 11th International Conference on Atherosclerosis Paris*, October 6, 1997, p. 398.
32 L. Charpentier and I. E. Murr, *Anal. Chim. Acta*, 1995, **318**, 89.
33 G. Lia, J. M. Liao, G. Q. Hu, N. Z. Ma and P. J. Wu, *Biosens. Bioelectron.*, 2005, **20**, 2140.
34 S. Aravamudhan, A. Kumar, S. Mohapatra and S. Bhansali, *Biosens. Bioelectron.*, 2007, **22**, 2289.
35 S. K. Arya, M. Datta, S. P. Singh and B. D. Malhotra, *Anal. Bioanal. Chem.*, 2007, **389**, 2235.